

10th CIRP Conference on Photonic Technologies [LANE 2018]

# Optical coherence tomography for laser transmission joining processes in polymers and semiconductors

Heiko Meyer<sup>a,\*</sup>, Mirsolav Zabic<sup>b</sup>, Stefan Kaieler<sup>a</sup>, Tammo Ripken<sup>a</sup>

<sup>a</sup>Laser Zentrum Hannover e.V., Hollerithallee 8, 30419 Hannover, Germany

<sup>b</sup>Leibniz Universität Hannover, Institute of Quantum Optics, Welfengarten 1, 30167 Hannover

\* Corresponding author. Tel.: +49 511 2788 231 ; fax: +49-511-2788-100. E-mail address: [h.meyer@lzh.de](mailto:h.meyer@lzh.de)

## Abstract

Laser transmission welding applications become wide spread technology in joining transparent and turbid materials. The requirement of higher throughputs and lesser rejects support the need of alternative methods to commonly used machine vision or temperature measurements. Optical coherence tomography delivers the opportunity to qualitatively assess transmission welding seams and welding spots even in three dimensions. Fourier Domain Mode Lock Lasers (FDMLs) used in OCT enable high throughput by high sweep rates. Preliminary results of OCT used for qualitative assessment of laser transmission welded polymers and fiber reinforced plastics are shown as well as first approaches of using OCT in a silicon chip bonding process.

© 2018 The Authors. Published by Elsevier Ltd. This is an open access article under the CC BY-NC-ND license

(<https://creativecommons.org/licenses/by-nc-nd/4.0/>)

Peer-review under responsibility of the Bayerisches Laserzentrum GmbH.

*Keywords:* OCT; laser transmission welding; quality control

## 1. Introduction

Due to the vast development of laser transmission welding approaches in joining processes of polymers, reinforced plastics and recently also semiconductors, non-destructive monitoring became a crucial topic in a variety of different production areas. Surveillance of process parameters, solo or in combination with a prior quality control of the join partners plays a crucial role in a sustainable product quality.

Current monitoring often relies on post process or in-line methods which are not able to give a qualitative and or quantitative process feedback. Optical coherence tomography (OCT) is well established in medical and industrial applications. However, whereas in medical monitoring, volumetric visualization is performed almost ever since OCT was developed, in most industrial applications OCT is mostly but widely applied 2D depth imaging or 3D contour control in metal welding applications. However recent research approaches [1] tend towards real 3D imaging approaches, especially in the field of laser transmission welding. Despite of a variety of alternative process control techniques, OCT is so far the only technique

providing real volumetric information of processed areas, thus, enabling not only subsequent assessment of transparent material structures (as e.g. welding seam and defects) but rather could be also applied as quality control device of the joining partners prior to the welding process in order to perform an in line welding parameter adjustment in case of defects in one or the other joining partner. OCT could easily provide this feature with a few microns resolution, thus being economically and technically advantageous in contrast to 1D and 2D process control techniques. Additionally, recent development approaches of Fourier Domain Mode Locked lasers (FDML) [2, 3] and Vertical Cavity Surface Emitting Lasers (VCSEL) [4] may provide new state of the art process control, by already delivering four times higher A-scan rates in contrast to current commercial available OCT sources in industrial process control for laser transmission welding applications but also for other industrial applications, wherever fast volumetric control devices are required due to evolving process speeds, as e.g. in welding processes or rather in growing numbers of parallel laser processed small devices, as e.g. in laser based eutectic bonding processes of semiconductor devices.

## 2. Materials and Methods

Instead of an ultra-fast 1550 nm FDML OCT source, first test measurements were performed with a commercially available swept source OCT System (OCS1300SS Thorlabs). The central wavelength of this system is 1325 nm with a spectral bandwidth of 100 nm. Axial resolution, which depends on central wavelength and spectral bandwidth, is 12 μm in air. With the build-in scan lens (LSM03 Thorlabs) the resulting transverse resolution is 15 μm. A schematic overview of the optical setup is depicted in Figure 1. The OCT signal is detected with a balanced photodetector that suppresses DC and autocorrelation noise in the interference signal. To avoid numerical k-space resampling a k-clock is used that acts as a sampling clock for the 14-bit digitizer. This prefiltered, in k-space linear signal is then evaluated with “Thorlabs Swept Source OCT Imaging System” Version 2.3.0.

The samples were placed on a stage below the scan lens. The integrated pilot laser beam (635 nm) showed the desired field of view (FOV), which was chosen so that a distinct area left and right of the welding seam was also taken into account. Thus, the FOV was set to 6 x 6 x 3 mm<sup>3</sup>.

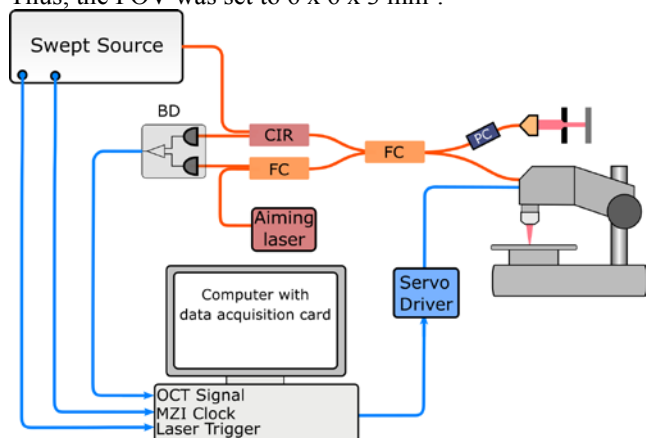


Fig. 1. Schematic overview of the optical setup. BD: Balanced Photodiode, CIR: Circulator, FC: Fiber Coupler, PC: Polarization Controller

Polymers, fiber reinforced plastics and semiconductor devices were produced in and/or kindly provided by cooperating groups within the Laser Zentrum Hannover. The corresponding transmission curves of PE, PPS, PEI and silicon (Si) are shown in figure 2 and figure 3 respectively. PPS and PEI were both reinforced with either short glass fibers or glass fiber fabric, resulting in an optically opaque appearance.

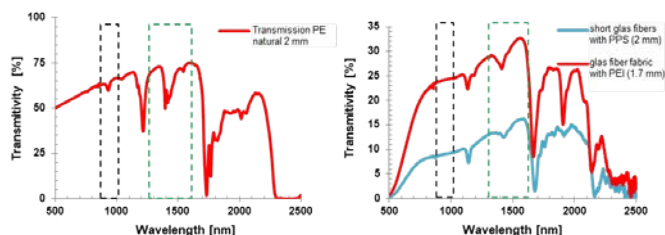


Fig. 2. Wavelength dependent transmittivity of 2 mm thick polyethylene (PE) (left) as well as short glass fibers containing polyphenylene sulfide (PPS) and glass fiber fabric reinforced polyethylenimine (PEI) (both right). The black dashed section shows the applications window for laser transmission welding, whereas the green dashed line represents the applied OCT source of 1325 nm

center-wavelength including also the range of the proposed 1550 nm OCT. In all presented cases it becomes obvious, that the wavelength region of the used and proposed OCT sources may reach a significant advanced penetration depth and thus, a better image quality in comparison to commonly used OCT sources ranging from 800 nm to 900 nm.

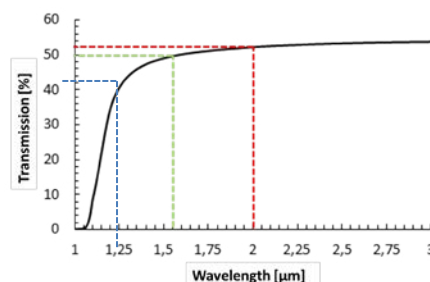


Fig. 3. Transmission spectra of silicon in the spectral range of 1 μm to 3 μm. The blue dashed line represents the used OCT center wavelength. The green line represents an OCT wavelength of 1550 nm for the application of e.g. FDMLs or VCSEL, whereas the red line shows the processing wavelength of 2 mm for laser induced micro bonding.

The major issue of imaging reinforced polymers with OCT arises through the high scattering effects in the material due to the construction of the polymers of different refractive indices, which is the limiting factor to the penetration depth (see fig. 4.).

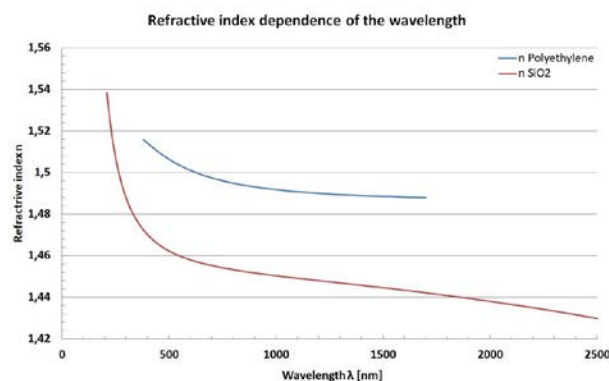


Fig. 4. Wavelength dependent refractive index of Polyethylene (blue) and SiO<sub>2</sub> (red).

The laser transmission welded samples consist of to joining partners of either PE/PE, PE/GFRP, PE/CFRP or GFRP/CFRP of roughly 10 cm ± 5 mm length each. The overlay of the joint section was approximately 4 cm ± 5 mm (fig. 5 shows exemplarily a sample of PE/CFRP).



Fig. 5. Laser transmission welded PE/CFRP sample.

The OCT B-Scan image (fig. 6), represents one section of a volume of the afore-mentioned volume. The joint area of the

two materials can clearly be identified. Additionally, small lesions and defects are clearly visible resulting in single spots due to refractive index mismatches and thus, refraction or due to absorption.

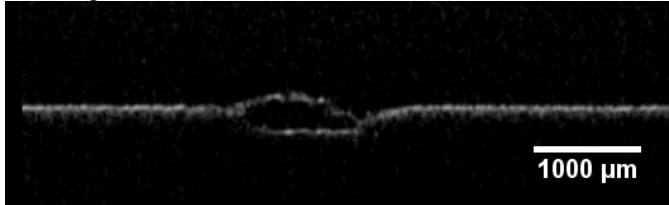


Fig. 6. OCT B-scan of a PE/PE sample. Observable are the welding seam itself, as well as small lesions in the upper joining partner.

All images were processed using ImageJ [5-7]. We have applied OCT volumetric imaging on various samples, ranging from thermoplastics (PE) to high end glass fiber fabric containing plastics (GFRP) and carbon fiber fabric containing plastics (CFRP) as well as on Si based RFID chips.

Subsequent microscopic images of micro sections of resin embedded samples (s. fig. 7.) were taken using a standard upright inspection microscope (Zeiss Stemi 2000 C equipped with a Zeiss AxioCam MRC) at 0.8 x and 5 x magnification.

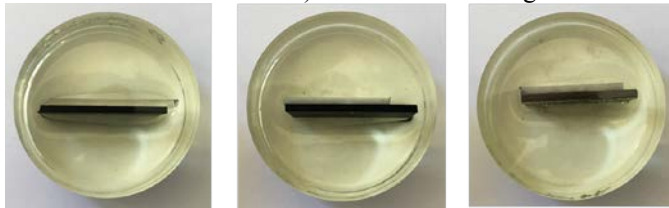


Fig. 7. Overview of resin embedded laser transmission welded samples. The first named material is always the upper joining partner, the second one consequently the lower joining partner. From left to right: PE/PE, PPS/PE and GFRP/CFRP.

### 3. Results

Usually, a welding seam is represented by an absent OCT signal [1]. However this can only occur, if the joining partners consist of the same material and thus the welding results in a homogeneous material distribution with minor yet measurable or rather no change in the index of refraction. In case of a non-measurable signal, this may depend on a lack of dynamic range of the OCT detector. However, as soon as varying materials or additives of different refractive index are used, the welding seam itself will be represented by a changed refractive index, thus, resulting in a clearly observable signal also with a reduced dynamic range of the system.

If all these parameters are known, both variations can be used as a criteria for the quality of the welding seams in laser transmission welding applications, and thus, as a quality assurance tool to replace destructive testing in a spot check. Additionally, this tool can be used not only as a quality control device, but rather a process control device, improving part handling, a priori product quality control and inline process control delivering a reliable response of the fabricated welding seam and the joint partners.

Figure 8 represents a depiction of the B-Scan of a PE/PE welded sample as well as the volume rendering of 6x6x3 mm volume. The total acquisition time was 10 seconds.

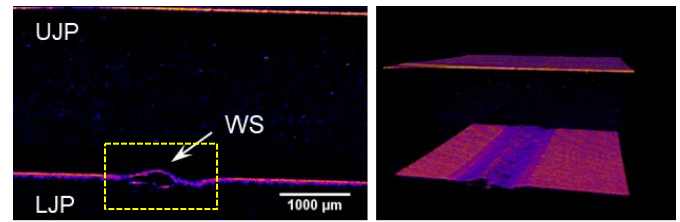


Fig. 8. OCT volume measurement of a laser transmission welded (LTW) Polymer-Polymer-sample of PE, whereas UJP represents the upper and semi opaque joint partner, WS is the welding seam and LJP the absorptive lower joint partner. The left depiction shows as single B-Scan whereas the right image shows a 3D rendering of a 6 x 6 x 3 mm<sup>3</sup> field of view using ImageJ.

In figure 9, we focused on the yellow outlined area of afore describe data set to perform a measurement of the welding seam with the FOV over the whole volume.

Therefore, we first resliced the volume along its longitudinal axis with subsequent application of a maximum intensity projection (MIP) adding all sections in one image. After binarisation of the MIP, we used a median filter to reduce artifacts from the material inhomogeneities and lesions finalized by an edge finding algorithm representing the outlines of the welding seam. The red dashed lines represent a mean thickness of the welding seam of  $258 \pm 38 \mu\text{m}$  (fig. 9).

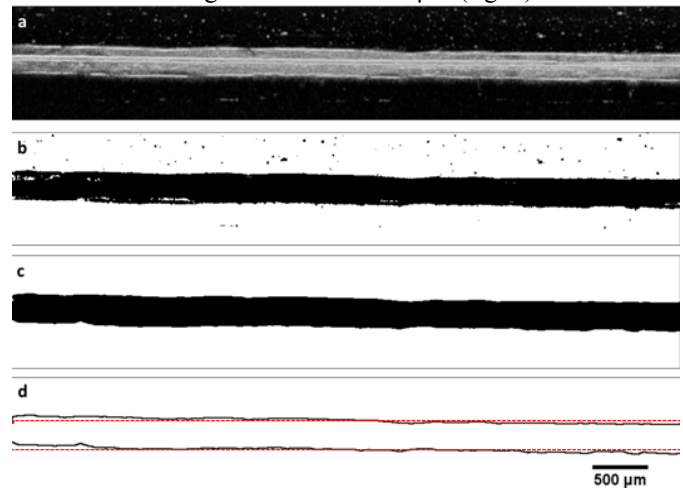


Fig. 9. OCT volume measurement on a laser transmission welded (LTW) of PE/PE welded samples, a) MIP of resliced volume, b) binarisation of a), c) applied median filter, d) edge finding of the outlines of the welding seam.

Fig. 10 represents the top view of the measured field of view of the welding seam of 6x6 mm<sup>2</sup>. Clearly observable are various curve shaped surface artifacts which show no affiliation with the welding seam. Additionally, the welding seam clearly rises from the background and can thus be measured *in silico* either directly or as applied here, after filtering.

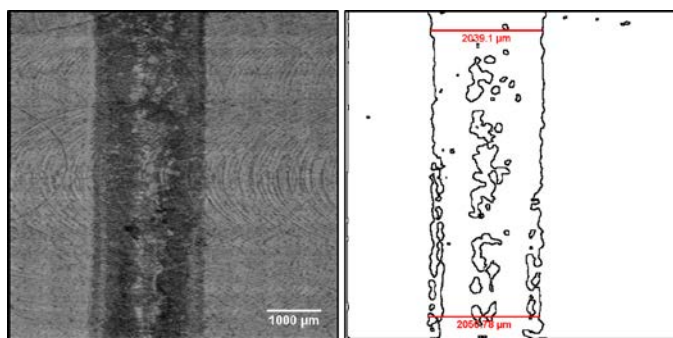


Fig. 10. Maximum Intensity Projection (MIP) of the welding seam applied to a PE/PE sample (left). Welding seam after binarisation, applying a median filter and an edge finding algorithm for the outlines.

Images of the micro sections were taken accordingly (fig. 11). It appears that the heat affect zone is not totally detectable with OCT. Interestingly the halo above the welding seam in the transparent joining partner is significantly visible in the micro section (s. fig. 11 right).

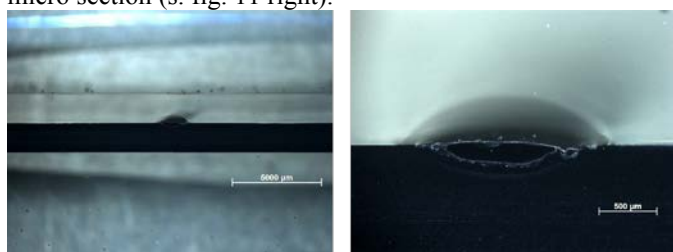


Fig. 11. Cross section of the PE/PE sample. Left, 0.8 x magnification and right, 5 x magnification. It is noticeable, that a slight halo occurs on above the welding seam, resulting as a change in the refractive index due to the heat affect zone.

An explanation could be an insidious change of the refractive index over the heat affect zone, thus resulting in an index gradient and therefore and due to the absence of a hard refractive index change, being not detectable for the OCT. However, the influence of the change in refractive index above and around the welding seam will cause distortions of the OCT beam and thus must be taken into account for quantitative measurements if desired. However, qualitative measurements of welding seams can still be performed. Additional measurements were performed on reinforced polymer samples as shown in fig. 12 and can be correlated with cross sections methods as in fig. 13.

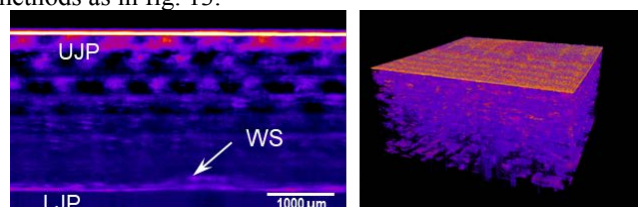


Fig. 12. OCT volume measurement on a laser transmission welded (LTW) GFRP-CFRP sample. UJP represents the upper and semi opaque joint partner (here GFRP, PEI with glass fiber fabric), WS is the welding seam and LJP the absorptive lower joint partner (here CFRP). Average intensity (AI) projection of 512 B-Scans (l.) and 3D rendering (r).

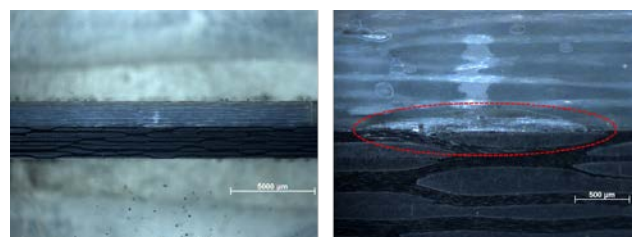


Fig. 13. Cross section of the GFRP/CFRP sample. Left 0.8 x magnification and right 5 x magnification. In contrast to the PE/PE sample, the heat affect zone appears to be significantly more homogeneous probably due to the high scattering coefficient of the GFRP effecting the intensity distribution of the welding beam.

To address a new field in laser based joining processes, we applied the same OCT in laser based eutectic bonding processes of semiconductor devices (fig. 14). According to fig. 3, we achieved approximately 45 % coupling efficiency into the Si based RFID chip, which was already enough, to acquire a strong OCT signal to visualize the internal structure of the RFID chip. Significant limitations will be metalized surfaces on semiconductors which cannot be penetrated by wavelengths in the NIR or MIR region. However, this limitation might be overcome by measuring volumetric stresses inside the RFID chip using polarization sensitive OCT as an indicator for sub metal-surface alterations, which is currently under investigation.

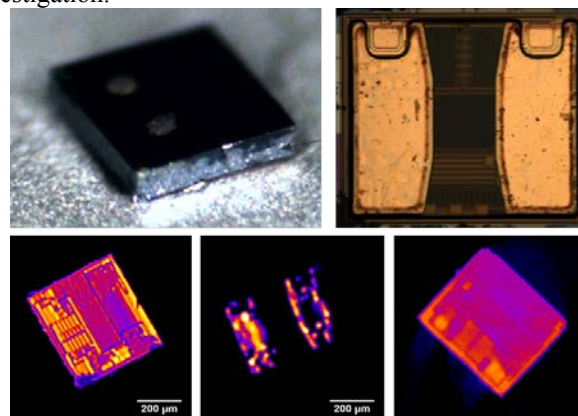


Fig. 14. OCT volume measurement of a Si based RFID Chip (upper left). MIP of the volume information of the top layer (bottom left) and the bottom layer (bottom center) and corresponding  $\mu$ CT volume of the same chip.

## Conclusion

Laser based joining processes have been established in industrial processes over decades and it is impossible to imagine one without the other. It has been shown that the OCT has the potential of being a versatile and powerful tool in non-destructive quality control and furthermore for *apriori* and in-line process control to amplify laser joining processes in the polymer manufacturing industry.

Due to the heat affect zone, it may be necessary to integrate smart algorithms in the reconstruction, since the change of refractive index affects the optical pathway of the incoupled OCT signal and the OCT detection signal. Thus, resulting distances can be error afflicted which has to be taken into account. However, it is clearly observable, that fabric reinforced plastics, which cover an already broad and still grow-

ing market, will be a challenge for current OCT devices to enable qualitative and quantitative measurements, due to the refractive index mismatch between the fabric and the polymer but also due to the densely packed mismatch. Concentrating on novel light sources or multi wavelength OCT approaches, addressing the optical dispersion of different materials, may result in suitable and applicable solutions to these problems.

Additionally, high flexibility and high throughput, as e.g. required by the automotive and/or semiconductor industry, can be achieved with high A-scan rates, resulting in high production rates. These novel sources already deliver up to 7 times the speed of currently commercial OCT sources. Swept Source OCT with Megahertz rates is currently possible with FDML-Lasers [2,3] and VCSEL [4]. A new interesting approach for ultrahigh speed OCT was published by Zhang et al. [8], who describes a new technique that utilizes an arbitrary waveform generator in combination with a Mach-Zehnder modulator for optically processing single A-scans with a rate of 10 MHz. Additional information may be achieved applying polarisation sensitive OCT to measure stress distortions with the material.

### Acknowledgements

The authors would like to thank the members of the CPM and the members of the MST group, both located at the LZH for providing the samples and for the fruitful discussions.

### References

- [1] Schmitt, R. and Ackermann, P., "OCT for Process Monitoring of Laser Trasmision Welding: Inline tracking of weld seams enables monitoring and quality control of polymer welding processes", *Process Monitoring, Laser Technik Journal*, 5/2016, pp15-18,
- [2] Zhi, Zhongwei, et al. "4D optical coherence tomography-based microangiography achieved by 1.6-MHz FDML swept source." *Optics letters* 40.8 (2015): 1779-1782.
- [3] Wieser, Wolfgang, et al. "High definition live 3D-OCT in vivo: design and evaluation of a 4D OCT engine with 1 GVoxel/s." *Biomedical optics express* 5.9 (2014): 2963-2977.
- [4] Potsaid, Benjamin, et al. "MEMS tunable VCSEL light source for ultrahigh speed 60kHz-1MHz axial scan rate and long range centimeter class OCT imaging." *Optical Coherence Tomography and Coherence Domain Optical Methods in Biomedicine XVI*. Vol. 8213. International Society for Optics and Photonics, 2012.
- [5] Rasband, W.S., ImageJ, U. S. National Institutes of Health, Bethesda, Maryland, USA, <https://imagej.nih.gov/ij/>, 1997-2016.
- [6] Schneider, C.A., Rasband, W.S., Eliceiri, K.W. "NIH Image to ImageJ: 25 years of image analysis". *Nature Methods* 9, 671-675, 2012
- [7] Abramoff, M.D., Magalhaes, P.J., Ram, S.J. "Image Processing with ImageJ". *Biophotonics International*, volume 11, issue 7, pp. 36-42, 2004.
- [8] Zhang, Xiao, et al. "Optical computing for optical coherence tomography." *Scientific reports* 6 (2016): 37286.